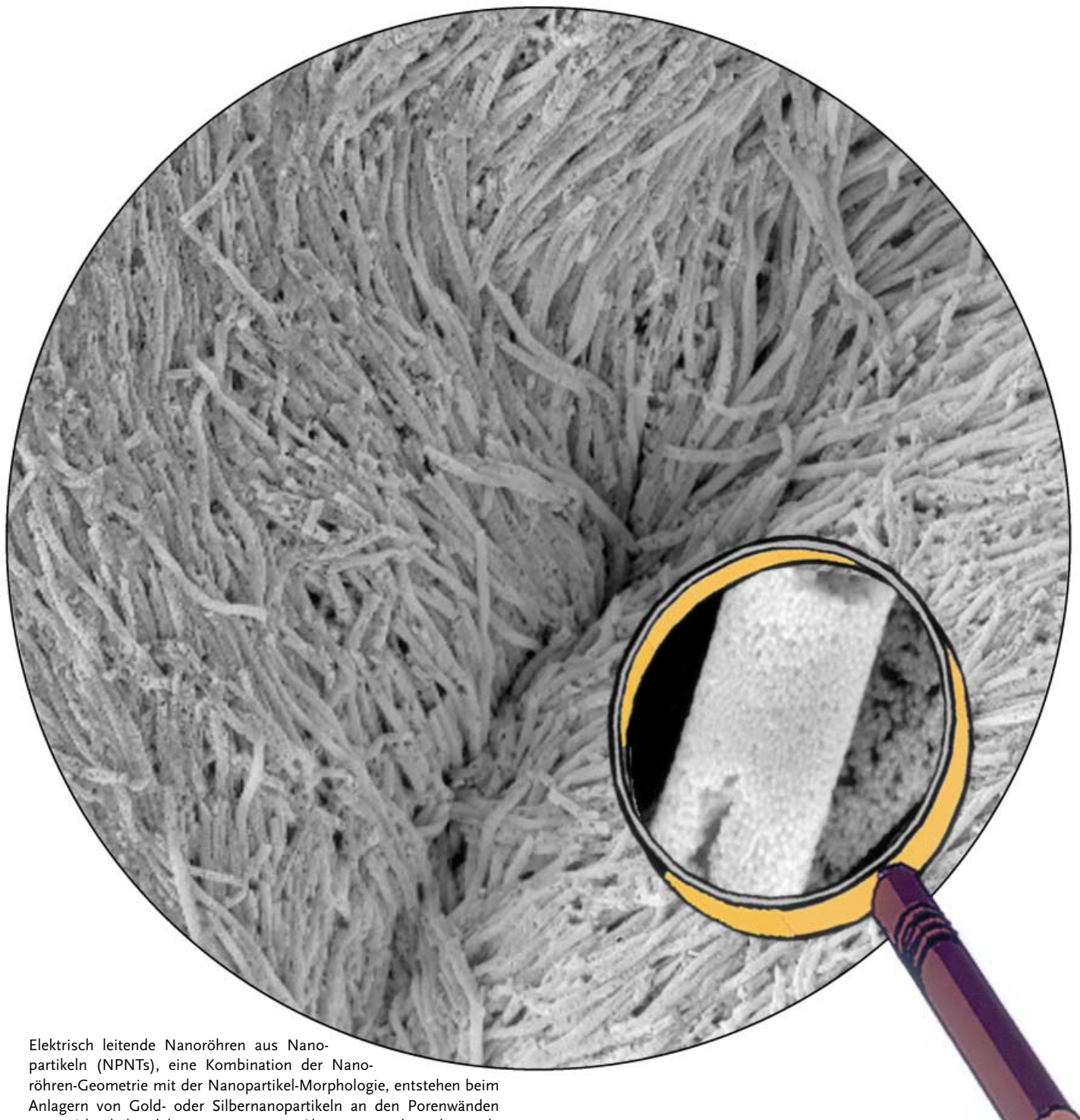# *Zuschriften*

Elektrisch leitende Nanoröhren aus Nano-
partikeln (NPNTs), eine Kombination der Nano-
röhren-Geometrie mit der Nanopartikel-Morphologie, entstehen beim
Anlagern von Gold- oder Silbernanopartikeln an den Porenwänden
einer Silan-behandelten nanoporösen Aluminiumoxidmembran als
Templat. Selbsttragende NPNTs können durch Auflösen des Templats
erhalten werden. Einzelheiten dazu sind in der Zuschrift von Rubin-
stein et al. auf den folgenden Seiten zu finden.

Nanoparticle Nanotubes**

Michal Lahav, Tali Sehayek, Alexander Vaskevich, and Israel Rubinstein*

In recent years there has been considerable interest in the synthesis of structured materials and control of their shape and geometry on different length scales, from molecular to macroscopic.[1,2] Special attention has been given to materials structured on the nanometer scale, representing a step down in size from present technology. Two prominent components of such systems are nanoparticles[3,4] and nanotubes.[5,6]

Nanoparticles, which are particularly attractive building blocks for nanomaterial architectures,[7] can be prepared from a variety of materials including metals,[8] semiconductors, and polymers.[4] Their dimensions, typically several to hundred nm, provide unique flexibility in the synthesis of composite nanomaterials. Examples include controlled aggregation in solution,[9] as well as binding to templates such as macromolecules,[10] and to solid substrates of planar[3,11] or curved[12] geometries. By using such methods a variety of self-sustained structures, including hollow spheres,[13] rods,[14] and chainlike multiparticle assemblies,[15] have been obtained. Binding of (sub)monolayer amounts of Au colloids to the pore walls of nanoporous alumina membranes was reported.[16,17]

Nanotubes of various kinds have been prepared in the last decade, starting from the discovery of carbon nanotubes by Iijima.[18] Recently other types of nanotubes have been produced, including metallic (e.g., Au), [19] other inorganic (e.g., TiO_2, HfS_2, V_7O_{16}, CdSe, MoS_2),[5,20–22] and polymeric (e.g., polyaniline, polyacrylonitrile) nanotubes.[23] These are synthesized by several methods,[5] including, for example, hydrothermal synthesis, surfactant-assisted synthesis, and decomposition in H_2 or electron radiation.

A common method for producing nanotubes is template synthesis in nanoporous membranes.[24,25] Template synthesis of nanotubes is achieved by using different strategies[26] such as electrochemical deposition, electroless deposition, polymerization, sol–gel deposition, or chemical vapour deposition (CVD) in the nanoporous templates.

Herein we present a novel synthetic procedure leading to a new kind of porous, high-surface-area "nanoparticle nanotube" (NPNT). The NPNTs are prepared by assembly of gold (or silver) nanoparticles on the pore walls of a silane-treated nanoporous alumina membrane template, accompanied by spontaneous room-temperature coalescence of the bound nanoparticles. Under well-defined conditions this process results in a solid tubular structure spanning the entire pore length. Self-sustained NPNTs, which preserve the nanoparticle morphology, are obtained by template dissolution.

Alumina membranes (about 220 nm average pore diameter) were pretreated with 3-aminopropyl trimethoxysilane (APMS) according to a reported procedure.[27] The silyl groups react with the hydroxyl groups on the alumina surface, thus leaving the amine groups available for binding Au nanoparticles. Au colloid solution (14 ± 2 nm diameter, citrate stabilized, prepared according to a literature procedure,[28] but with five times the original concentrations of the starting materials) was then passed through the modified membrane pores by vacuum suction (Figure 1). Au nanoparticles interact with the amine groups of the APMS and
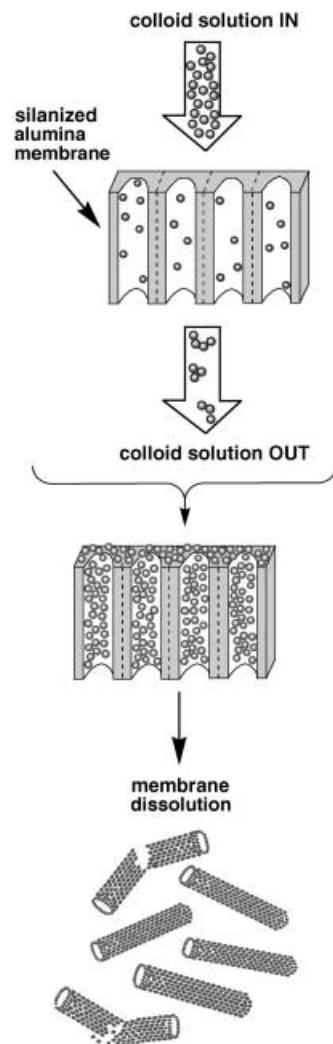
[*] Prof. I. Rubinstein, Dr. M. Lahav, T. Sehayek, Dr. A. Vaskevich
Department of Materials and Interfaces
Weizmann Institute of Science
Rehovot 76100 (Israel)
Fax: (+972) 8-934-4137
E-mail: israel.rubinstein@weizmann.ac.il

Supporting information for this article is available on the WWW under http://www.angewandte.org or from the author.

Figure 1. Schematic diagram showing the preparation of metal NPNTs. A nanoparticle solution is passed through a silanized alumina membrane, followed by membrane dissolution (dimensions are not to scale).

become immobilized on the pore walls, similar to the process observed on flat surfaces.[3,11] The Au nanoparticle arrangement in the membrane pores is visualized by cross-section environmental scanning electron microscope (ESEM) imaging of the membrane following colloid binding, as shown in Figure 2a. The nanoparticles are seen as bright spots on the pore walls. Note that no nanoparticle immobilization is observed when the same process is carried out with membranes that have not been silanized.

In marked contrast with Au nanoparticle binding to amino-terminated flat surfaces in stagnant solutions,[3,11] immobilization on the pore walls under the present conditions is not restricted to the first layer of nanoparticles. Continued flow of the colloid solution through the pores promotes

additional nanoparticle binding and formation of a multilayer structure. The immobilization is assumed to involve aggregation of surface-confined Au nanoparticles accompanied by spontaneous coalescence (possibly during membrane drying) to yield continuous, solid NPNTs. Although the NPNT formation mechanism is not yet fully understood, partial stripping of the citrate stabilizing shell on the Au nanoparticles may be the primary step in the immobilization, rearrangement and coalescence.[13,15,29]

Dissolution of the colloid-treated (and dried) alumina membrane in 1.0 M NaOH followed by removal of the solution led to the release of solid, self-sustained Au NPNTs. Figure 2b–d and Figure 3 show ESEM and transmission electron microscope (TEM) images, respectively, of the
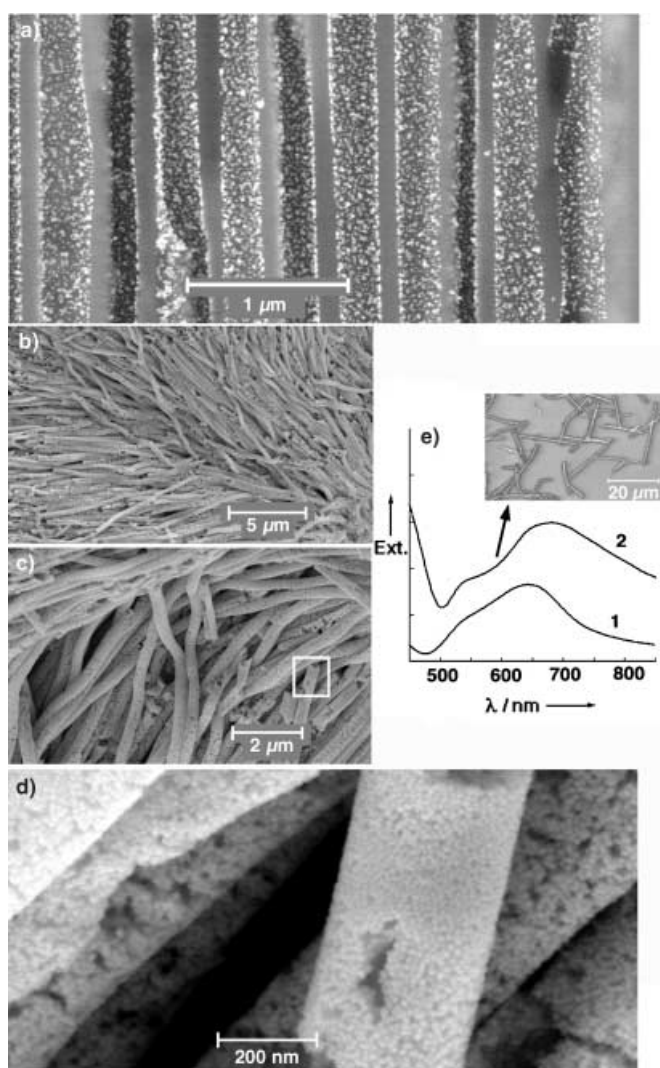

Figure 2. a) ESEM image showing the cross-section of a silanized nanoporous alumina membrane after passing a Au nanoparticle solution and drying. b–d) ESEM images of Au NPNTs obtained after alumina membrane dissolution in 1.0 M NaOH, shown at different magnifications. d) A magnified image of the area marked in (c), showing the arrangement of individual nanoparticles. e) Transmission UV/Vis spectrum (extinction versus wavelength) of Au NPNTs in solution (1) and on a glass slide (2). Inset: ESEM image of the sample used for obtaining spectrum (2).
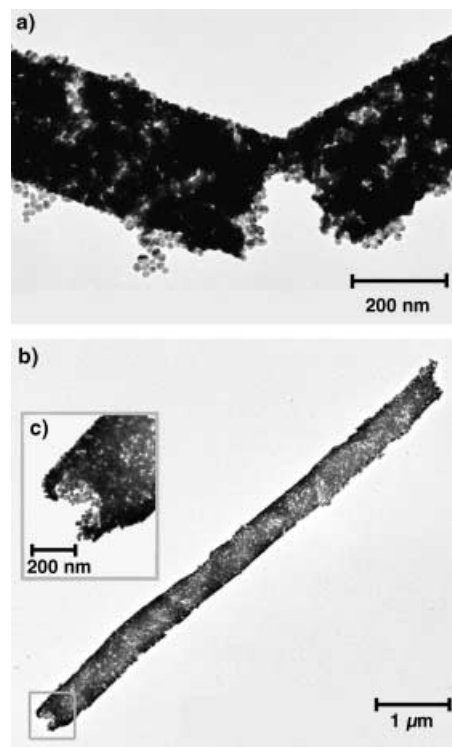

Figure 3. a) and b): TEM images of NPNTs obtained after alumina membrane dissolution in 1.0 M NaOH, shown at different magnifications. c) A magnified image of the area marked in (b), showing the tubular structure.

free-standing nanotubes, presented at different magnifications. The nanotubes are composed of a continuous, multi-layered nanoparticle array. Some nanotubes are partly bent as a result of the dissolution and drying (Figure 2b, c), which indicates limited mechanical strength. Defects are frequently seen along the nanotubes, but the geometrical shape is preserved. Electron diffraction (not shown) produced a pattern characteristic of an assembly of randomly-oriented Au crystallites.

The process of NPNT formation can be observed by passing an increasing volume (5–18 mL) of Au nanoparticle solution through the surface-modified alumina membrane. Figure 4a–c presents ESEM images taken at different stages
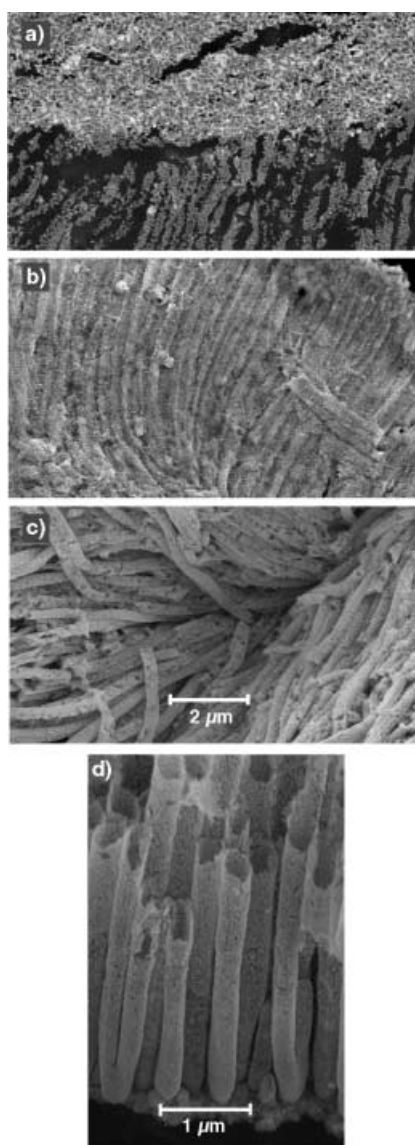
Figure 4. NPNT development and modification. (a–c) ESEM images showing the progress of Au NPNT formation after passing a) 5 mL, b) 9 mL, c) 18 mL of Au nanoparticle solution, followed by drying and membrane dissolution. d) ESEM image of Au NPNTs after Cu electrodeposition and membrane dissolution.

of NPNT formation, obtained after membrane dissolution. At the initial stage (5 mL) most of the nanoparticles appeared as random aggregates (Figure 4a, top), with sporadic appearance of elongated structures that survived membrane dissolution (Figure 4a, bottom). When more nanoparticles (9 mL) were passed through the membrane, a rather fragile nanotube arrangement resulted (Figure 4b), whereas when the maximal amount in these experiments was used (18 mL), fully developed, mechanically stable, multilayered NPNTs were produced (Figure 4c).

In contrast with the system reported by Steinhart et al.[30] in which annealing was necessary to convert Pd nanoparticles formed on membrane walls to nanotubes, the opposite effect was observed with the spontaneously formed Au NPNTs. Hence, membranes with fully grown NPNTs were annealed

(220°C, 17 h) followed by membrane dissolution. ESEM imaging (not shown) revealed severely damaged nanotube fractions, which arise from local conversion of nanoparticle aggregates into large, separated lumps.

Transmission UV/Vis spectroscopy of the NPNTs was carried out both in solution (Figure 2e, line 1) and with a sample dried on a glass slide (Figure 2e, line 2). The weak extinction band at about 530 nm is attributed to a small amount of free nanoparticles. The more intense band, attributed to the NPNTs, appears at longer wavelengths, characteristic of nanoparticle aggregates. The latter is shifted more to the red in the dry sample (about 675 nm) versus the wet sample (about 645 nm) and this shift is due to the different media, different orientations of the nanotubes in the solution and on the slide, and possibly a structural change (additional aggregation) upon nanotube drying. The dry sample was also imaged by ESEM (Figure 2e, inset) to confirm the presence of Au NPNTs on the glass slide.

The NPNTs are electrically conductive and show perfect ohmic behavior with no hysteresis. A resistance of about 0.3 ohm·cm^2 was measured across the nanoparticle-modified membrane (see Experimental Section); the apparent specific resistivity, $\rho \approx 6$ ohm·cm, was calculated by using the overall NPNT wall thickness and ignoring the interconnected nanoparticulate structure. The NPNT electrical conductivity can be used to modify their chemical, structural, and mechanical properties by using electrodeposition. In the present case a small amount of copper was electrodeposited on the NPNTs following Au colloid immobilization and prior to membrane dissolution.[31] The presence of Cu along the tubes was confirmed by energy dispersive spectroscopy (EDS) measurements (see Supporting Information). Figure 4d shows ESEM side view of the hybrid NPNTs after membrane dissolution. A well-ordered assembly of continuous, rigid, hollow, Cu-covered nanotubes is observed. The Cu-modified NPNTs are considerably more robust than the pristine Au NPNTs, as evident in the cross-sectional images (compare Figure 2a, with Supporting Information). Careful inspection suggests that most of the defects are "repaired" by the deposited Cu, while the basic nanoparticulate structure is maintained.

The procedure for producing Au NPNTs can be adopted with other metals, by replacing the Au colloid solution with, for example, a solution of citrate-stabilized Ag nanoparticles. This results in self-sustained Ag NPNTs (see Supporting Information).

In conclusion, a novel procedure is presented, providing metal "nanoparticle nanotubes" (NPNTs) that combine nanotube geometry with nanoparticle morphology and properties (e.g., high surface-to-volume ratio; surface plasmon optical absorption). The process involves passing a metal (Au, Ag) colloid solution in the pores of a surface-modified nanoporous alumina membrane, followed by spontaneous room-temperature coalescence of the surface-confined nanoparticles to yield solid, multilayered nanotubes. These nanotubes can be obtained as free-standing NPNTs by dissolution of the membrane template. The mechanism of NPNT formation is not yet fully understood and is currently being studied. The new process opens the way to the synthesis of novel kinds of nanomaterials that have a tube geometry, high

surface area, mechanical stability, electrical conductivity, and distinct optical properties. The synthesis of various new types of NPNTs, for example, other metal NPNTs, as well as more complicated structures such as bimetallic NPNTs, is being investigated.

Modification of the NPNT properties can be achieved by exploiting their electrical conductivity for electrochemical deposition on the nanotube surface, as exemplified here with Cu coating. This, as well as possible chemical (electroless) deposition, enables formation of composite NPNT systems that have modified mechanical, electrical and optical properties, as well as diverse surface chemistries. These unique properties of NPNTs may be particularly useful in catalysis and electrocatalysis,[32] as well as in sensing, microfluidic, chemistry-on-a-chip, binding of biological molecules, and future device applications.

Experimental Section

NPNT synthesis: Au NPNTs were prepared as follows: 18 mL (unless otherwise specified) of Au nanoparticle solution were passed by vacuum suction through the silanized alumina membrane (Whatman, Anodisc 0.2 µm) by using the following procedure: (1) 10 mL of the red nanoparticle solution was passed through the membrane (note: the first 5–6 mL coming out of the membrane are colorless, the remaining amount comes out colored). (2) The membrane was sonicated for 4 min. (3) A few mL of triply distilled water were passed through the membrane. (4) An additional 8 mL of Au nanoparticle solution was passed through the membrane. (5) Distilled water was passed through the membrane (an indication that the nanotubes are not blocked). The membranes were then dried under a stream of nitrogen. To obtain self-sustained NPNTs the alumina membrane was dissolved in 1.0 M NaOH over 2.5 h then washed with triply distilled water.

Samples for UV/Vis spectroscopy: A NPNT solution was prepared by dissolving the colloid-treated alumina membrane in 1.0 M NaOH, followed by removal of the solution and redispersion of the NPNTs in water. The dry sample was prepared by applying a drop of the NPNT solution on a cleaned microscope cover slide followed by evaporation of the solution.

NPNT conductivity: A gold contact layer (100 nm thick) was evaporated on both faces of the Au nanoparticle-modified membrane, avoiding the membrane edges. The membrane resistivity was then measured using a cyclic voltage scan. An apparent specific resistivity (ρ) of the NPNTs was estimated by using the following values: a measured resistance of 0.3 ohm·cm^2 across the membrane; a membrane pore density of 10^9 cm^{-2}; a pore diameter of 220 nm; a membrane thickness of 60 µm; a NPNT wall thickness (estimated from ESEM images, ignoring the nanoparticluate morphology) of 40 nm. A control experiment with a similar membrane that was not exposed to a Au nanoparticle solution showed infinite resistance.

Cu electrodeposition: The membrane was mounted in a special holder, leaving the "outlet" side (bottom side of the membrane in Figure 1, middle) in contact with a Cu^{2+} solution (0.3 M CuSO$_4$ + 0.1 M H$_2$SO$_4$).[31] Electrical connection (cathode) was established by contacting the "inlet" side of the alumina membrane, covered with bound Au nanoparticles (Figure 1). A standard electrochemical cell was used with a K$_2$SO$_4$-saturated Hg/Hg$_2$SO$_4$ (MSE) reference electrode and a Pt counter electrode. Electrodeposition was carried out at −0.8 V (versus MSE) for 60 s.

[1] D. L. Feldheim, C. D. Keating, *Chem. Soc. Rev.* **1998**, *27*, 1–12.
[2] S. I. Stupp, V. LeBonheur, K. Walker, L. S. Li, K. E. Huggins, M. Keser, A. Amstutz, *Science* **1997**, *276*, 384–389.
[3] R. G. Freeman, K. C. Grabar, K. J. Allison, R. M. Bright, J. A. Davis, A. P. Guthrie, M. B. Hommer, M. A. Jackson, P. C. Smith, D. G. Walter, M. J. Natan, *Science* **1995**, *267*, 1629–1632.
[4] A. N. Shipway, E. Katz, I. Willner, *Chemphyschem* **2000**, *1*, 18–52.
[5] C. N. R. Rao, M. Nath, *J. Chem. Soc. Dalton Trans.* **2003**, *1*, 1–25.
[6] R. Tenne, A. K. Zettl, *Top. Appl. Phys.* **2001**, *80*, 81–112.
[7] P. C. Hidber, W. Helbig, E. Kim, G. M. Whitesides, *Langmuir* **1996**, *12*, 1375–1380.
[8] D. L. Feldheim, C. A. Foss in " *Metal Nanoparticles*", Marcel Dekker, New York-Basel **2002**, p. 338.
[9] C. A. Mirkin, R. L. Letsinger, R. C. Mucic, J. J. Storhoff, *Nature* **1996**, *382*, 607–609.
[10] R. Djalali, Y. Chen, H. Matsui, *J. Am. Chem. Soc.* **2002**, *124*, 13660–13661.
[11] A. Doron, E. Katz, I. Willner, *Langmuir* **1995**, *11*, 1313–1317.
[12] A. Dokoutchaev, J. T. James, S. C. Koene, S. Pathak, G. K. S. Prakash, M. E. Thompson, *Chem. Mater.* **1999**, *11*, 2389–2399.
[13] S. Chah, J. H. Fendler, J. Yi, *J. Colloid Interface Sci.* **2002**, *250*, 142–148.
[14] J. T. Hu, T. W. Odom, C. M. Lieber, *Acc. Chem. Res.* **1999**, *32*, 435–445.
[15] Z. Y. Tang, N. A. Kotov, M. Giersig, *Science* **2002**, *297*, 237–240.
[16] T. Hanaoka, H. P. Kormann, M. Kroll, T. Sawitowski, G. Schmid, *Eur. J. Inorg. Chem.* **1998**, 807–812.
[17] S. M. Marinakos, L. C. Brousseau, A. Jones, D. L. Feldheim, *Chem. Mater.* **1998**, *10*, 1214–1219.
[18] S. Iijima, *Nature* **1991**, *354*, 56.
[19] M. Wirtz, M. Parker, Y. Kobayashi, C. R. Martin, *Chem. Eur. J.* **2002**, *8*, 3573–3578.
[20] T. Kasuga, M. Hiramatsu, A. Hoson, T. Sekino, K. Niihara, *Langmuir* **1998**, *14*, 3160–3163.
[21] M. Worle, F. Krumeich, F. Bieri, H. J. Muhr, R. Nesper, *Z. Anorg. Allg. Chem.* **2002**, *628*, 2778–2784.
[22] R. Tenne, *Colloids Surf., A*, **2002**, *208*, 83–92.
[23] L. Feng, S. H. Li, H. J. Li, J. Zhai, Y. L. Song, L. Jiang, D. B. Zhu, *Angew. Chem.* **2002**, *114*, 1269–1271; *Angew. Chem. Int. Ed.* **2002**, *41*, 1221–1223.
[24] C. R. Martin in *Electroanalytical Chemistry, Vol. 21* (Eds.: A. J. Bard, I. Rubinstein), Marcel Dekker, New York **1999**, pp. 1–74.
[25] C. John, C. R. Martin, *J. Mater. Chem.* **1997**, *7*, 1075–1087.
[26] R. A. Caruso, J. H. Schattka, A. Greiner, *Adv. Mater.* **2001**, *13*, 1577–1579.
[27] C. A. Goss, D. H. Charych, M. Majda, *Anal. Chem.* **1991**, *63*, 85–88.
[28] J. Turkevich, P. C. Stevenson, J. Hiller, *Discuss. Faraday Soc.* **1951**, *11*.
[29] N. A. Alcantar, C. Park, J. M. Pan, J. N. Israelachvili, *Acta Mater.* **2003**, *51*, 31–47.
[30] M. Steinhart, Z. Jia, A. K. Schaper, R. B. Wehrspohn, U. Gösele, J. H. Wendroff, *Adv. Mater.* **2003**, *15*, 706–709.
[31] T. Sehayek, A. Vaskevich, I. Rubinstein, *J. Am. Chem. Soc.* **2003**, *125*, 4718–4719.
[32] A. Cho, *Science* **2003**, *299*, 1684–1685.